International Journal of Green Management and Business Studies
Vol. 1, No. 1. December 2021
THE SCIENCE PUBLISHING HOUSE

Green-Economic Constructions Using Composite GFRP Closed Forms

Hamdy M. Mohamed
Department of Civil and Architectural Engineering, College of Engineering, Applied Science University (ASU), Kingdom of Bahrain/London South Bank University (LSBU), London, UK.
Hamdy.mohamed@asu.edu.bh

Abstract
Green and Sustainability are big words these days. Recently, the demand for more green construction or sustainable construction has been driven largely by consumers in the construction sector. In this study, new filament wound glass fiber-reinforced polymer (GFRP) tubes are used as an FRP-stay in place structural formwork for concrete beams. The test results of an experimental study carried out on 230 mm diameter and 2000 mm long concrete filled FRP tubes (CFFTs) beams are presented. Three CFFT beams and two control specimens without tube were tested under four-point bending. One control specimen was reinforced with steel spirals of stiffness equivalent to the GFRP tube and the other had no transverse reinforcement. The parameters used in this investigation include the effect of laminate thickness of FRP tubes, the type of the internal reinforcements (steel or GFRP bars) and the type of transverse reinforcements (spiral steel or FRP tubes). The fiber orientations of the tubes were mainly in the hoop direction. The two control specimens failed in shear; however, using GFRP tubes instead of transverse steel reinforcement changed the mode of failure of the three CFFT beams to flexural failure. In addition, the GFRP tubes confine the concrete core which subsequently increases the ultimate compression capacity and the ductility of the specimens. Also, test results indicate that the GFRP tube enhances the flexural strength of the specimens, whereas it provides a longitudinal reinforcement in the tension side.

Keywords: Green, Beam; Concrete; Flexural; Fiber-Reinforced Polymer; Tubes.

1. Introduction

Corrosion of steel reinforcement causes continual degradation to the infrastructures in worldwide and it has prompted the need for challenges to those involved with reinforced concrete structures. Sustainable construction aims at reducing the environmental impact of a building of its entire lifetime, while optimizing its economic viability. The benefits of green construction are many; lower operating costs, increased asset value, reduced waste sent to landfills, conservation of energy and water, and reduced greenhouse gas emissions, for example. In the last decade, considerable efforts have been made to apply fibre-reinforced polymers (FRP) composites in the construction industry, and recently, structural applications of FRP composites started to appear in civil infrastructure systems. FRP products are a cost-effective material choice in many green construction circumstances. Furthermore, as their international recognition and reputation as an ecologically sustainable product continues to grow, so do the uses and applications.

Available online: ***www.scipubhouse.com***

FRP composite materials have been used as internal and external reinforcement in the field of civil engineering constructions. It has been used as internal reinforcement for beams, slabs and pavements (Masmoudi et al., 1998); (Rizkalla et al., 2003), and also as external reinforcement for rehabilitation and strengthening different structures (Demers & Neale, 1998). Recently, the use of FRP tubes as structurally integrated stay-in-place forms for concrete members, such as beams, columns, bridge piers, piles and fender piles has emerged as an innovative solution to the corrosion problem. In such integrated systems, the FRP tubes may act as a permanent form, often as a protective jacket for concrete, and especially as external reinforcement in the primary and secondary directions such as for confinement. Furthermore, the use of concrete filled-FRP tubes (CFFTs) technique is predicated on performance attributes linked to their high strength-to-weight ratios, expand the service life of structures, enhance corrosion resistance, and potentially high durability (Mirmiran & Shahawy, 1996); (Mirmiran et al., 2000); (Seible et al., 1999); (Fam, Green, et al., 2003), and (Fam, Pando, et al., 2003); (Zhao et al., 2004)).

In fact, extensive research programs have been conducted to investigate the behaviour of concrete columns confined with FRP sheets and FRP tubes under pure compression load. However, relatively few studies have focused on static flexural strength of CFFTs (Mirmiran et al., 2000); (Davol et al., 2001); (Fam & Rizkalla, 2003). To date, only two studies have been reported in the literature on flexural behaviour of CFFT beams reinforced with longitudinal FRP or steel bars (Fam, Green, et al., 2003); (Cole & Fam, 2006). The experimental test results of five reinforced CFFT and two RC beams indicated that CFFT beams performed substantially better than beams with a steel spiral. Unlike CFFTs with FRP rebar, CFFTs with steel rebar failed in a sequential progressive manner, leading to considerable ductility and strength (Cole & Fam, 2006). Also, it was concluded that the most critical parameter affecting the behaviour of steel reinforced CFFT beams was steel reinforcement ratio: when increased, it improved stiffness, strength, and ductility. Furthermore, (Cole & Fam, 2006) reported that increasing the proportion of fibres in the axial direction of the tube or increasing concrete compressive strength tends to increase strength and stiffness, only after yielding of rebar. The test results of aforementioned RCFFT and control beams of (Cole & Fam, 2006) with new two prestressed CFFT beams were included in another study by (Fam, Green, et al., 2003). It was found that the strength of control specimens was governed by crushing and spalling of concrete cover. Also, unlike spiral reinforcement, GFRP tubes confined larger concrete areas and also contributed as longitudinal reinforcement, leading to increases in flexural and shear strengths, up to 113% and 69%, respectively.

The objective of present study is to examine the flexural behaviour of reinforced CFFT circular beams. New GFRP tubes were used to act as stay-in-place formwork for beams. The fibre orientations of these tubes were mainly in the hoop direction. The experimental investigation included a total of five beam specimens, approximately 213 mm in diameter and 2.00 m in length, tested in four-point bending. In the following sections, full details about the experimental program of this study and the considered parameters are provided as well as the analysis of experimental test results.

2. Methodology

2.1 Materials

Green Composite FRP Bars: Sand-coated glass bars manufactured by a Canadian company [ADS Composites/Pultrall Inc., Thetford Mines, Quebec], with a fibre content of 73% in vinyl ester resin, were used. The bars were made of continuous fibres (glass) impregnated in a vinyl ester resin using the pultrusion process. The GFRP bars #5 were used as longitudinal reinforcement for CFFT beams. The tensile properties of the FRP bars were determined by performing tensile tests on representative. Table 2 presents the mechanical properties of the FRP bars.

Green Composite FRP Tubes*:* New Glass-fibre reinforced polymer (GFRP) tubes were used as structural stay in place formwork for the CFFT specimens of this study. Two different types of the GFRP tubes namely D and E were used with different thicknesses and having the same diameters. The tubes were manufactured using continuous filament winding process adopted by FRE Composites, St-Andre-d'Argenteuil, Quebec, Canada. E-glass fibre and Epoxy resin were utilized for manufacturing these tubes. The glass fibre volume fraction as provided by the manufacture was 68% ± 3%. The internal diameter for the two tubes equals 213 mm, the thickness of tube D equals 2.90 mm, while for tubes E was 6.40 mm. The thickness of tube E was almost double of tube D. Different fibre angles with respect to the longitudinal axis of the tubes were used (±60°, ±65°, ±45°, 90°). It is clear that the fibre orientations of the tubes were mainly in the hoop direction, and no fibres in the longitudinal direction. The winding angles of the tubes D were optimized for below underground pipe applications, while tubes E were designed for pipe telecommunication applications. The tubes were provided with a total length equal to 6000 mm. Table 3 shows the details of fibre orientations, stacking sequences, thickness and internal diameter for each type of the tubes. For each type of FRP tubes, ten coupons cut from the untested sections were tested under uniaxial tension followed (ASTM, 2008), "Tensile properties of Plastics". The tensile coupons dimensions were prepared according the specification of the standard to provide an adequate gripping area at each end.

The width of specimen at the grip length was more than that of the free length. Figure 1 shows the details and dimension of FRP tube coupon specimens. The stress-strain relationships are presented in Figure 2 for the two FRP tubes, at the first stage of loading the curves were linear up to 80% of the peak load. Beyond this level the curves were nonlinear up to failure. Small load drops accompanied by the change in the stiffness were observed. This resulted from the earlier rupture of fibres and matrix cracking. The ultimate tensile stress ranged from 56 MPa to 60 MPa, while the axial strain at the peak stress ranged from 0.004 to 0.005.

Concrete: All specimens in this study were constructed from one concrete batch named (N). The target strength of batch N was intended to provide normal concrete strength of 30 MPa. Concrete batch was supplied by ready mix concrete supplier. The maximum size of the coarse aggregates was about 20 mm. Ten plain concrete cylinders (152 x 305 mm) were prepared from concrete batch and cured under the same conditions as the test specimens. Five cylinders were tested in compression after 28 days. The 28-day average concrete compressive strength was found equal to

30 ±0.6. The remaining five cylinders were tested in tension by performing the split cylinder test. The average tensile strength ranged from 3.0 to 3.4 MPa.

Steel bars: In this study, two different steel bar diameters were used to reinforce the CFFT and control specimens under flexural loads. Mild steel bars of 3.4 mm diameter were used as spiral reinforcement for the control specimens. Deformed steel bars No. 15M was used for CFFT beams. The mechanical properties of the steel bars were obtained from standard tests that were carried out according to (ASTM, 2009) A615/A615M-09, on five specimens for each type of the steel bars. The actual properties are given in Table 1 in terms of diameter, nominal area, yield and ultimate strength and young's modulus.

Table 1. Properties of reinforcing steel bars.

Bar type		Diameter (mm)	Nominal Area (mm^2)	Yield strength (MPa)	Ultimate strength (MPa)	Modulus of elasticity (GPa)
Size	Type					
Wire	Mild Steel	3.4		675	850	221
15M	Deformed	16.0 200 419	686	200		

Table 2. Properties of reinforcing FRP bars

US size	Type	Nominal diameter (mm)	Nominal area (mm^2)	Tensile modulus of elasticity (GPa)	Ultimate tensile strength (MPa)	Ultimate strain (%)
#5	GFRP	15.875	198	48.2	683	1.8±0.06

Table 3. Dimension and details of the GFRP tubes

Tube type	Internal diameter (mm)	Thickness (mm)	Number of layers	Stacking sequence
D	203	2.90	6	$[60, 90_4, 60]$
E	203	6.40	12	$[\pm 60_2, 90_2, \pm 60_2, 90_6]$

(a) Specimen dimension

(b) Tests setup

Figure 1: Test procedures for coupon tension test

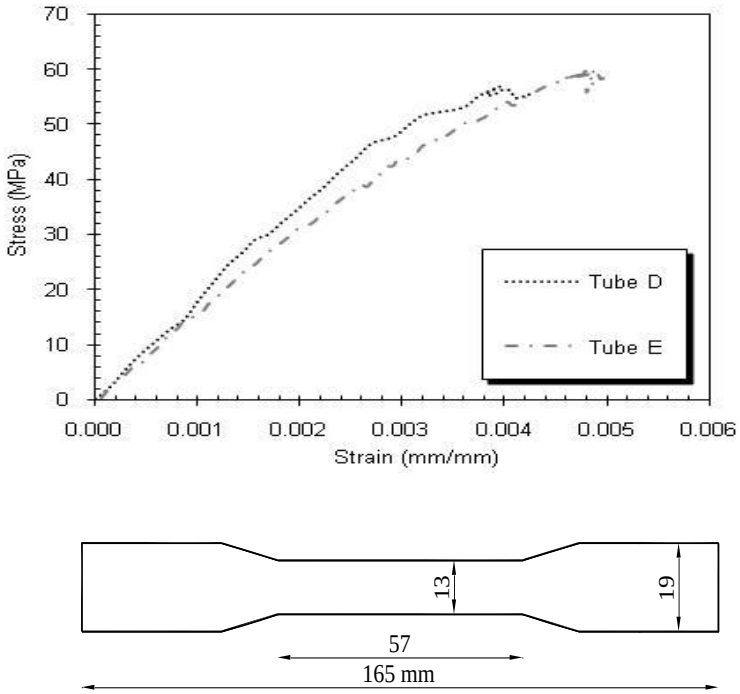

Figure 2: Stress-strain behaviour of the FRP tubes for the coupon tensile test

2.2 Specimens

The test matrix included five beams, one conventional reinforced concrete (RC) circular beams without spiral reinforcement and one RC beam with spiral reinforcement, while the remaining three specimens were RCFFTs. The specimens of each series were reinforced with steel or glass FRP bars with the same reinforcement ratio, 0.76%. Normal concrete compressive strength (N) was used in order to cast the beam specimens. Table 4 shows the details of RC and RCFFTs beams including their identification, height, diameter, type of internal reinforcements and concrete strength.

Table 4. Test matrix and details of beam specimens

Tube type	Diameter (D=mm)	Shear reinforcement	4t/D%	Flexural reinforcement	Internal reinforcement ratio
CO-S-N	203	---	-	Steel bars	3.65 (6No. 15)
COS-S-N	203	Steel spiral	-	Steel bars	
D-S-N	213	Tube D	4.5	Steel bars	
D-G-N	213	Tube D	4.5	GFRP bars	
E-G-N	213	Tube E	12.6	GFRP bars	

The specimens were identified by codes listed in the first column of Table 4. The identifications CO and COS are used for control conventional RC beams without and with spiral reinforcement, respectively. The terms D or E indicate the type of the used FRP tube for the beam based on Table 3. The second letters indicate the type of flexural reinforcement, whereas, S or G means steel or glass FRP bars, respectively, was used for the specimen. The terms N is used to indicate the type of concrete used to cast the specimens. The beam specimens were designed to study the effects of several parameters, and were compared to each other as follows:

- Evaluating the contribution of FRP tubes to the flexural capacity, compared to conventional RC beams with and without steel spiral reinforcement. Specimens D-S-N was compared to the control specimens (CO-S-N and COS-S-N). The RC beams without spiral reinforcements were compared to the RCFFTs specimens to determine the pure contribution of using FRP tube to the flexural capacity. On the other hand, the RC beams with spiral reinforcements were introduced to show the enhancement in the flexural capacity by using RCFFTs specimens. However, the spiral reinforcement was designed to provide approximately the same stiffness in the hoop direction as compared to the stiffness of tube type D.

- The effect of type of the internal reinforcements on the flexural performance of RCFFT beams. Steel and Glass FRP bars of the same cross sectional area (ϕ 15) were used in reinforcing concrete beams. Specimen D-S-N was compared to the specimen (D-G-N).
- The effect of the FRP tube thickness was studied through the specimens (D-G-N and E-G-N). The FRP tube type E has thickness (6.40 mm), which it is almost equal to two times the thickness of the tube type D, (2.90 mm). The laminate structure of the two tubes was almost the same, however, the fibres oriented in the hoop direction at 60 and 90 degree as compared to the longitudinal axes of the tubes.

The FRP tubes were cut to the proper length (2.00 m), as shown in Figure 3, using saw and then were cleaned and dried carefully. The FRP tubes provided the formwork for beam specimens. The control specimens were prepared for vertical casting using stiff cardboard tubes. The cardboard tubes were attached with four vertical stiffeners using wood plate of 50 x 30 mm, cross section distributed at the perimeter of the tube. Reinforcement cages with different configuration were constructed from glass FRP and steel bars. The rebar cage was designed to have an outside diameter of 193 mm, allowing for 10 mm clear spacing on all perimeters of the FRP tubes, which has a 213 mm internal diameter. The cages of the RCFFT specimens had six longitudinal bars (glass FRP bars or steel bars ϕ15). The longitudinal bars were held in its positions at equal intervals using three hoop steel stirrup (3.4 mm diameter) at the two ends and middle length of the cages. Figure 4 shows the typical steel and glass FRP cages which had been used to reinforce the RCFFT and control beam specimens.

Figure 3: Green FRP tubes for beam specimens

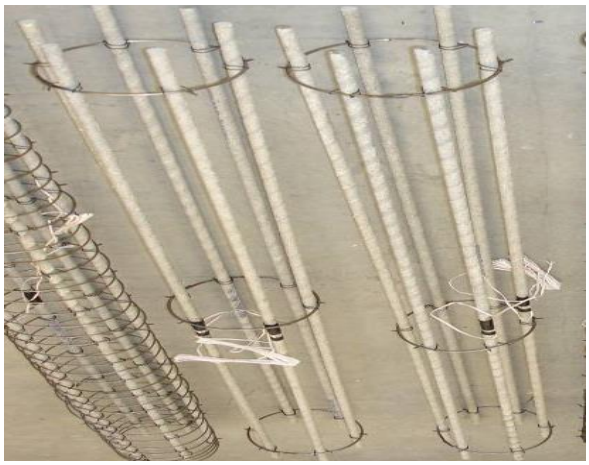

Figure 4: Typical steel and glass FRP cages

2.3 Measurements and Test Setup

The deflections were measured using three LVDTs at the mid-span and at each quarter-span to monitor the deflection profile along the beams. Two high-accuracy LVDTs (± 0.001 mm) were installed at the mid-span to measure the crack width. Also, one LVDT was attached at each support, to measure beam end rotations. In addition, two high-accuracy LVDTs (± 0.001 mm) were installed at the end of the beams to measure the slip between concrete core and FRP tube. The specimens were tested in four-point bending over a simply supported clear span of 1920 mm, see Figure 5. The load was transferred from the actuator to the tested beam at two points through a steel spreader I-beam applied on the round surface of the beams through curved loading plates on one-third diameter of the beam. A roller support was obtained by placing a steel cylinder between two steel flat plates. A pin support was obtained by using specially adapted steel I-beam. The upper plate of the I-beam had spherical groove and the plate was supported on the web plate which had a spherical end to house the plate and allow the rotation. Curved steel plated were connected at the top of the pin and roller supports, to cradle the beams against side movement, see Figure 5. During the test, the load was monotonically applied at a stroke controlled rate of 0.8 mm/minute using a 500 kN closed-loop MTS actuator.

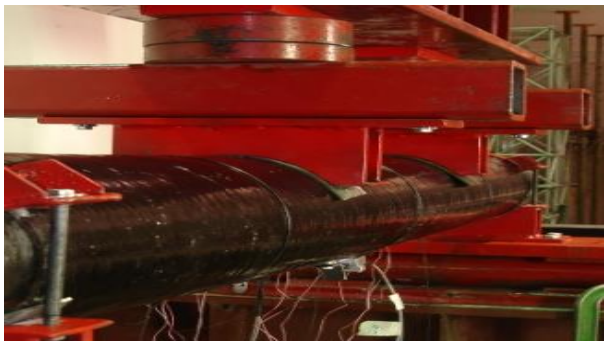

Figure 5: Overview for the test setup

3 Test Results and Discussions

3.1 General Behaviour

The three RCFFT beams failed in the tension side due to the tensile rupture of FRP tubes and reinforcing steel or FRP bars. While the two reinforced concrete beams without and with steel spiral reinforcement failed in shear and shear compression, respectively. A summary of the beam test results is presented in Table 5. The applied load at flexural cracking, the yield load, the ultimate load, the mid-span deflection and end support rotation at ultimate load, the maximum strain in the longitudinal bars, FRP tubes and concrete, and the failure modes are given in Table 5. It should be noted that each beam was symmetrically loaded with two concentrated loads and consequently, the applied load is the sum of the two concentrated loads.

3.2 Cracking and Yield Loads

Flexural cracks were initiated in the region of constant moment between the two concentrated loads. Table 5 gives the applied load at the initiation of flexural cracking for each tested beam. Figure 6 show the moment- curvature relationships for the RC and RCFFT beams. In Figure 6 the curvatures are calculated using the top and bottom longitudinal strains measured on the surface of the FRP tube. The corresponding curvature of the section, Ψ, which is the slope of the strain profile, is calculated as:

$$\Psi = \frac{\varepsilon_b - \varepsilon_t}{D} \quad (1)$$

Where ε_b and ε_t are the tensile and compressive strains of the bottom and top fibre of the tube.

Table 5. Test results of RC and RCFFT beams

Specimen ID	Load (kN)			Moment (kN.m)			Curvature ($\mu\varepsilon$/mm)		Comp strain* ($\mu\varepsilon$)	Deflection* (mm)	Failure mode**	Ductility (kN.m)
	Crack	Yield	Max	Crack	Yield	Max	Crack	Max				
CO-S-N	11.99	77.7	102.65	3.84	24.86	32.85		35	2633	11.99	DT	0.78
COS-S-N	12.14	82.5	152.97	4.88	26.40	48.95	1.00	216	3959	136.25	SC	17.75
D-S-N	19.88	116.3	236.71	6.36	37.21	75.75		112	15516	124.91	FL	32.40
D-G-N	15.90	---	144.79	5.09	---	46.33	3.01	93	6017	43.13	FL	5.78
E-G-N	17.34	---	177.14	5.55	---	56.68	2.02	100	6479	38.68	FL	8.77

Figure 6 shows that the first cracking in the concrete occurs at a relatively low load level, compared to the ultimate load. The cracking load ranged between 11.99 and 12.14 kN for the RC beams and ranged between 15.90 and 19.88 kN for the RCFFT beams. These values are

approximately 7.50 to 11.68% of the ultimate load. It can be noticed from Table 5 that there is a difference in the flexural cracking load. For each series, the beam reinforced transversely with FRP tube cracked at a load higher than that of the beam reinforced with steel spiral reinforcement or without.

The average cracking loads of beams reinforced with steel spiral reinforcement or without are 88.5 that of the beams reinforced with FRP tubes for specimens. This difference in the flexural cracking load may be attributed to the positive contribution of the FRP tubes to increase the axial stiffness of the beam as compared with steel spiral reinforcement beams. Also, the RCFFT beams reinforced with steel bars cracked at a load higher than that of the RCFFT beams reinforced with FRP bars. The average cracking load of RCFFT beams reinforced with steel bars is 81% that of the RCFFT beams reinforced with FRP bars. This difference in the flexural cracking load may be attributed to the difference in the axial stiffness of the longitudinal reinforcement. Table 5 gives the yield load for the RC and RCFFT beams reinforced with steel bars. The yield load for RC beams without and with steel spiral reinforcement (CO-S-N and COS-S-N) occurred at 75 and 54% of the ultimate load, respectively. The yield load for the beam reinforced with FRP tube Type D (D-S-N) yielded at load higher than that of the beam reinforced with steel spiral reinforcement (COS-S-N) which, in turn, had a higher yield load of the beam without transverse reinforcement (CO-S-N). The yield load for the beam reinforced with steel spiral reinforcement (COS-S-N) is 70% that of the beam reinforced with FRP tube Type D (D-S-N) and the corresponding value for the beam without transverse reinforcement (CO-S-N) is 66%.

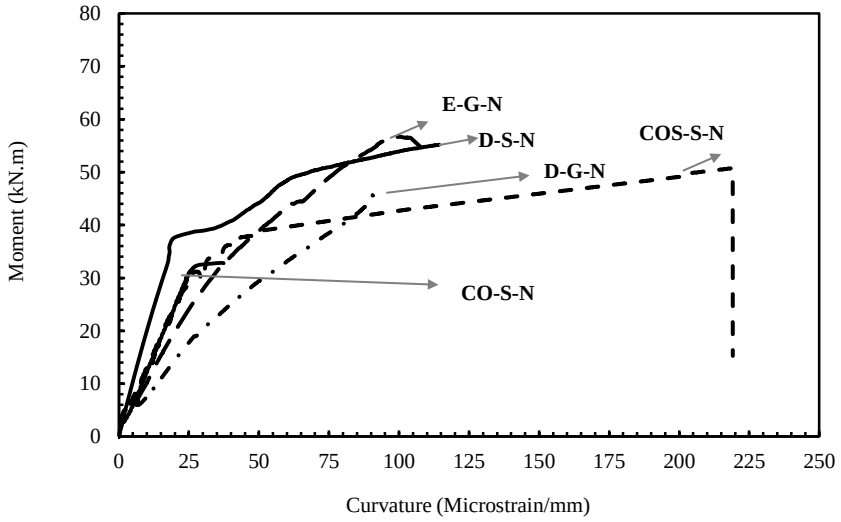

Figure 6 Moment-curvature relationships for RC and RCFFT beams

4 Effect of Test Parameters on Flexural Strength and Ductility

4.1 Effect of type of transverse reinforcement

The influence of the confinement using steel spiral or FRP tubes on the flexural strength and ductility of the tested beams is shown in Figures 7.a and 7.b, respectively. The GFRP tube has

increased the ultimate strength significantly and also improved the energy absorption capacity. This is attributed to two important aspects: The tube has a reinforcing effect in the longitudinal direction, which is not provided by the steel spirals, and also has a confining effect on the concrete core that is more effective than the steel spirals because the tube is located at the outermost surface and thus confines a larger concrete area. The figures indicate that the increase in the flexural strength and energy absorption for the steel-RCFFT beams are 55% and 82%, respectively, higher than the beam reinforced with a steel spiral for specimens. On the other hand, the increase in the flexural strength and energy absorption for the FRP-RCFFT beams are 9 and 7%, respectively, higher than the beam reinforced with steel spiral specimens. It can be observed that the improvement in the strength and energy absorption is not clear for beam reinforced with glass FRP bars, which may be attributed to the low modulus of elasticity of the glass FRP bars compared to steel bars. However, for the two series, using FRP tubes changed the mode of failure from shear (beam with and without steel-spiral) to flexural failure.

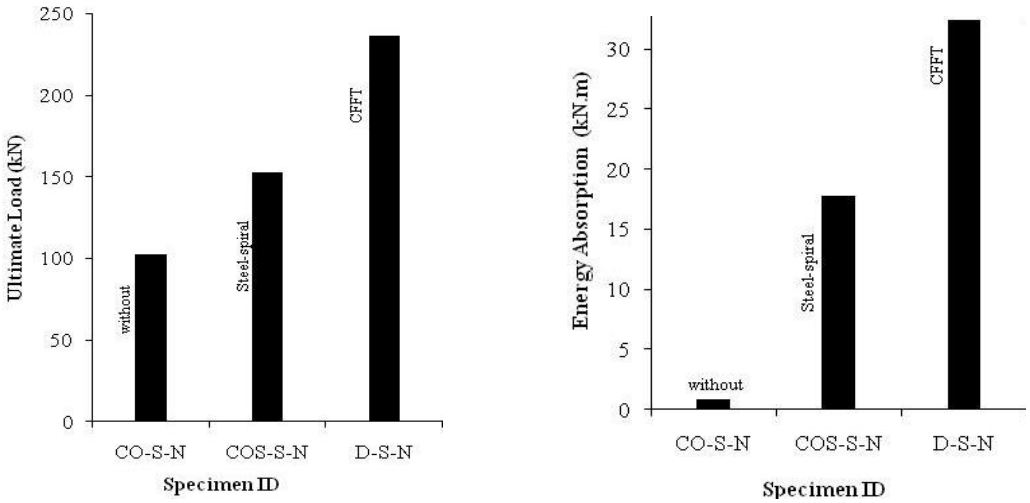

(a) (b)

Figure 7 Effect of type of transverse reinforcement on (a) Strength and (b) the energy absorption

4.2 Effect of type of longitudinal reinforcing bars

Figure 8 present the effect of type of the internal reinforcements on the flexural strength and energy absorption of tested RCFFT beams. The vertical axis in Figures 8.a and 8.b represents the flexural strength and the energy absorption, respectively, while the horizontal axis represents the effect of the type of longitudinal reinforcement as measured by the Young's modulus. Steel and Glass FRP bars of the same cross sectional area were used in reinforcing CFFT beams. Figure 8.a shows that the ratio of the strength of FRP-RCFFT beams to that of steel-RCFFT beams was 60%. This ratio approximately equals the cube root of axial stiffness ratio between glass and steel bars $\sqrt[3]{\rho_{fl} E_{fl} / \rho_{sl} E_{sl}}$. This result is consistent with the test results conducted by El-Sayed et al. 2006 on reinforced concrete beams without stirrups and reinforced in the longitudinal direction with glass FRP, carbon FRP and steel bars. The increase in the flexural strength for steel-RCCFTs

beams is attributed to the difference in the Young's modulus between the steel and GFRP bars. On the other hand, Figure 8.b shows that the energy absorption of the RCFFT beams reinforced with steel bars on average are 460% higher than that of beams reinforced with GFRP bars. This is attributed to the elastic-plastic behavior of the steel bars as compared with the linear elastic behavior of FRP bars. This result reflects the effect of the modulus of elasticity of the reinforcing bars on the flexural strength as well as the ductility of the RCFFT beams.

4.3 Effect of reinforcement ratio of FRP tubes

The effect of FRP tube reinforcement ratio on the flexural strength and energy absorption is presented in Figures 9.a and 9.b, respectively. The horizontal axis in Figures 9.a and 9.b represents the FRP tube reinforcement ratio as measured by the area of the tube divided by the area of the concrete core, $4t_{FRP}/D$. The four beams had identical reinforcement ratio of the GFRP bars, while the FRP tube reinforcement ratios ranged from 6 to 13%. It can be noticed that the flexural strength and energy absorption increased as the FRP tube reinforcement ratio was increased by using tube Type E instead of tube Type D. The FRP tube Type E has thickness (6.40 mm), which it is equal to 2.2 times the thickness of the tube type D, (2.90 mm). Figure 9 shows that increasing the FRP tube reinforcement ratio by 120% (from 5.44 to 13%) increased the flexural strength and the energy absorption on average by 20 and 58%. It is clear that the increase in the flexural strength (20%) is not significant as compared by the increase in the FRP tube reinforcement ratio (120%). This is attributed to the increase in the flexural strength is mainly resulted from the contribution of the increase in the thickness of the FRP tubes in the tension side of the beams. While the increase in the thickness of the FRP tubes in middle zone and compression side is attributed to increase the shear and compressive strengths of the beams. This was evidence as no crushing and shear failure occurred for all the RCFFT beams compared to steel-spiral RC beams. On the other hand, it is found that the average ratio of the experimental flexural strength is equal to the 3.5 root of the axial stiffness ratio (axial modulus of elasticity multiplied by the FRP tube thickness) between the two tubes, $\sqrt[3.5]{(E_{fl}t_{FRP})_{tube\,No.2}/(E_{fl}t_{FRP})_{tube\,No.1}}$, where tube No.1 has smaller thickness.

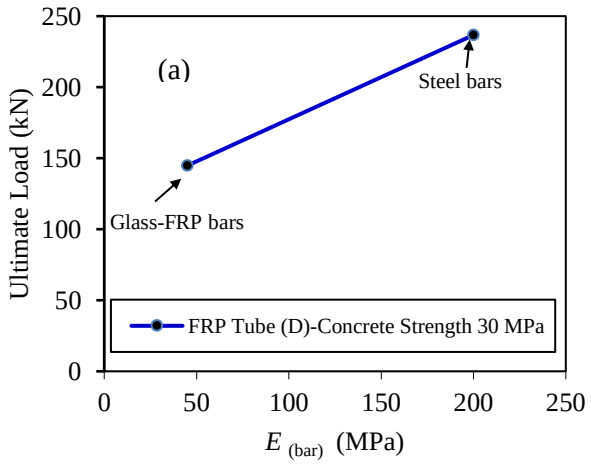

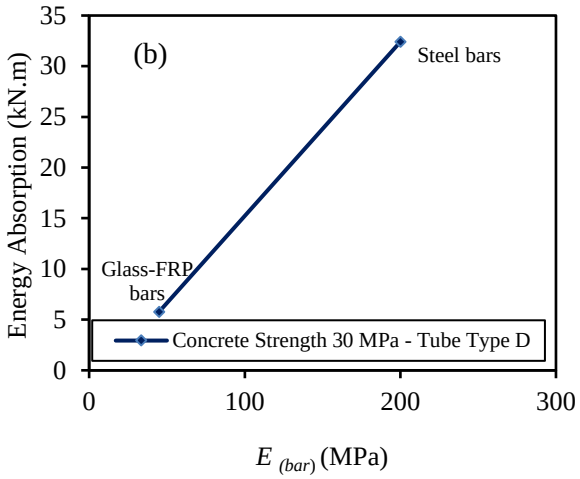

Figure 8 Effect of type of longitudinal reinforcements on (a) strength and (b) the energy absorption

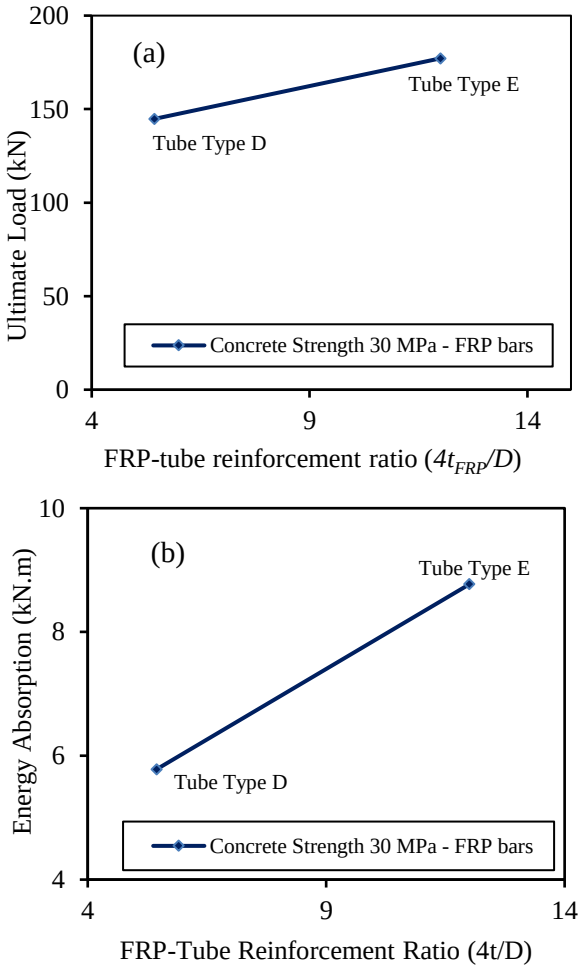

Figure 9 Effect of reinforcement ratio of FRP tubes on (a) strength and (b) the energy absorption

5 Conclusion

All the CFFT beams tested to failure in this study, failed in flexural. The prevailing flexural mode of failure was the tensile rupture of the FRP tube in the longitudinal direction with ruptures the reinforcing bars in the tension side. However, diagonal tension failure at the shear span and shear compression failure were the final failure modes for the RC control beams without and with spiral steel, respectively. This indicated that the FRP tube changed the mode of failure from shear to flexural failure. All the CFFT beams reinforced with steel or FRP bars exhibited progressive and sequential failure manner, leading to a remarkable pseudo-ductile behaviour. The experimental test results indicated that the beams confined by FRP tubes experienced lower deflection, higher cracking load level, higher ductility, higher stiffness and superior strength than the beam reinforced with a spiral-steel.

References

ASTM. (2008). *Standard Test Method for Tensile Properties of Plastics, D 638-08*. West Conshohocken.

ASTM. (2009). *Standard Specification for Deformed and Plain Carbon Steel Bars for Concrete Reinforcement, A615/A615M-09*. West Conshohocken.

Cole, B., & Fam, A. (2006). Flexural Load Testing of Concrete-Filled FRP Tubes with Longitudinal Steel and FRP Rebar. *Journal of Composites for Construction*, *10*(2), 161–171.

Davol, A., Burgueno, R., & Seible, F. (2001). Flexural Behaviour of Circular Concrete Filled FRP shells". *Journal of Structural Engineering*, *127*(7), 810–817.

Demers, M., & Neale, K. W. (1998). Confinement of Reinforced Concrete Columns with Fibre Reinforced Composite Sheets–an Experimental Study. *Can. J. Civ. Eng*, *V. 26*, 226–241.

Fam, A., Green, R., & Rizkalla, S. (2003). Field Application of Concrete-filled FRP Tubes for Marine Piles. *ACI Special Publication*, *SP-215-9*, 161–180.

Fam, A., Pando, M., Filtz, G., & Rizkalla, S. (2003). Precast Composite Piles for the Route 40 Bridge in Virginia Using Concrete-filled FRP Tubes. *PCI Journal*, *48*(3), 32–45.

Fam, A., & Rizkalla, S. (2003). Large Scale Testing and Analysis of Hybrid Concrete/Composite Tubes for Circular Beam-Column Applications. *Construction and Building Materials*, *V. 17*, 507–516.

Masmoudi, R., Thériault, M., & Benmokrane, B. (1998). Flexural Behaviour of Concrete Beams Reinforced with Deformed Fibre Reinforced Plastic Reinforcing Rods. *ACI Structural Journal*, *95*(6), 665–676.

Mirmiran, A., & Shahawy, M. (1996). New Concrete-Filled Hollow FRP Composite Column. *Composites Part B: Engineering*, *27B*(3–4), 263–268.

Mirmiran, A., Shahawy, M., el Khoury, C., & Naguib, W. (2000). Large Beam-Column Tests on FRP filled Composite Tubes. *ACI Structural Journal*, *97*(2), 268–276.

Rizkalla, S., Hassan, T., & Hassan, N. (2003). Design Recommendations for the use of FRP for Reinforcement and Strengthening of Concrete Structures. *Journal of Progress in Structural Engineering and Materials*, *5*(1), 16–28.

Seible, F., Karbhari, V. M., & Burgueno, R. (1999). King Stormwater Channel and I-5/Gilman Bridges. *Structural Engineering International*, *9*(4), 250–253.

Zhao, L., Burgueno, R., Rovere, H. L., Seible, F., & Karbhari, V. M. (2004). *Preliminary Evaluation of the Hybrid Tube Bridge System*.